Pflügers Arch. 375, 219–228 (1978)

Pflügers Archiv
European Journal
of Physiology

The Extracellular Patch Clamp: A Method for Resolving Currents through Individual Open Channels in Biological Membranes

Erwin Neher[1], Bert Sakmann[1], and Joe Henry Steinbach[2]

[1] Abteilungen Molekularer Systemaufbau und Neurobiologie, Max-Planck-Institut für Biophysikalische Chemie, Am Fassberg, D-3400 Göttingen, Federal Republic of Germany

[2] Neurobiology Department, The Salk Institute, P.O. Box 1809, San Diego, California 92112, U.S.A.

Abstract. The current contributions of individual ionic channels can be measured by electrically isolating a small patch of membrane. To do this, the tip of a small pipette is brought into close contact with an enzymatically cleaned membrane of a hypersensitive amphibian or mammalian muscle fiber. Current flowing through the pipette is measured. If the pipette contains cholinergic agonist at μ-molar concentrations, square pulse current waveforms can be observed which represent the activation of individual acetylcholine-receptor channels. The square pulses have amplitudes of 1 to 3 pA and durations of 10–100 ms.

In order to obtain the necessary resolution, a delicate compromise had to be found between different experimental parameters. Pipettes with 1–3 μm internal diameter and a steep final taper had to be used, extensive enzyme treatment was necessary, and conditions had to be found in which channels open at a relatively low frequency.

Key words: Receptor – Cholinergic – Ionic channels – Voltage clamp – Membrane current – Muscles.

Introduction

It has been known for some time that individual open ion-conducting channels in artificial membranes generally contribute square "pulses" of current: the transitions from one conductance state to another are very rapid relative to the average lifetime of the conducting state (Bean et al., 1969; Hladky and Haydon, 1972; Gordon and Haydon, 1972). This is to be expected on physical chemical grounds, since transition states in chemical reactions are short-lived. However, it has been impossible to resolve the currents flowing through individual channels in biological membranes. We have devised a method for recording such low amplitude events and have applied it to studies of the acetylcholine receptor on skeletal muscle fibers.

The acetylcholine receptor channel ('channel') was chosen for several reasons. First, its properties have been extensively studied by other techniques. These studies have shown that individual channels have a relatively large conductance (20–35 pS) and can have a relatively long duration (10–100 ms) e.g. Katz and Miledi, 1973; Colquhoun et al., 1975; Neher and Sakmann, 1976 b. Second, channels can be activated by chemical rather than electrical stimuli, simplifying the experiments. Finally, it is possible to obtain a suitably low frequency of channel opening events by using a low concentration of agonist and by studying the receptors present at low density in the extrajunctional membrane of denervated skeletal muscle fibers.

The following paragraphs describe the experimental methods used to measure currents through single channels, and present an evaluation of the technique. In addition, we present some properties of currents through single open channels, which are related to methods questions. A short account of part of this work has been previously published (Neher and Sakmann, 1976 a).

The Method

Experimental Arrangement

Intracellular records of membrane currents have a high background noise, because the Johnson voltage noise in the high resistance voltage sensing electrode is combined with the low input impedance of the cells. Even in the favourable case of small myotubes the minimum root mean square (rms) background noise was 30 pA (Sachs and Lecar, 1977), still one or two orders of magnitude larger than the current through a single open

0031-6768/78/0375/0219/$2.00

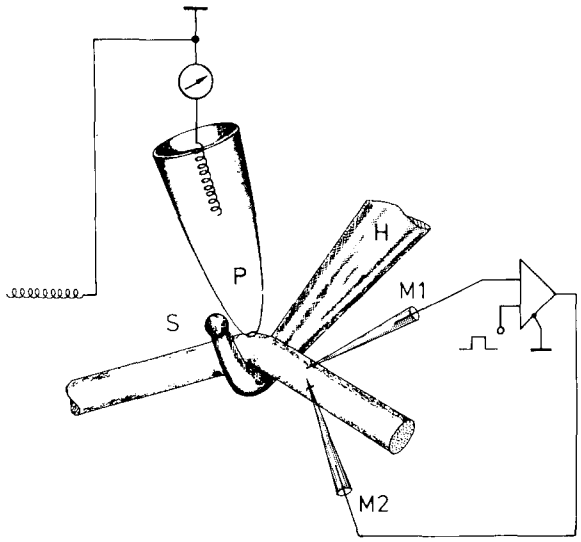

Fig. 1. Schematic drawing of mechanical fiber support and electrode placement. The fiber is lifted up by a glass look *H*, which also carries a ball of cured Sylgard *S* on its tip. Microelectrodes (*M1* and *M2*) and pipette *P* are placed within 50–100 μm of the supporting hook

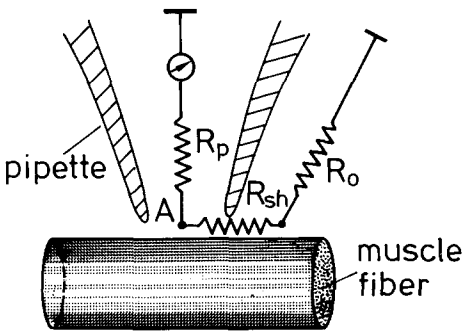

Fig. 2. Equivalent circuit for the extracellular space in the region of contact between muscle fiber and glass pipette (in cross section). R_p internal resistance of the pipette; R_{sh} resistance of the shunt pathway between pipette interior and bath fluid; R_o resistance between the cell surface and bath ground. The muscle fiber is considered to be an insulator. Opening of a channel in the patch area is modelled as a current injection from an ideal (high internal resistance) current source into the circuit at point A

channel in the experimental range of membrane potentials (e.g., Anderson and Stevens, 1973). The approach adopted by us to reduce the background current noise was to electrically isolate a small patch of membrane. This procedure reduced the endogenous membrane current noise since the impedance of the small patch of membrane under study is much higher than the input impedance of a whole fiber. Electrical isolation was accomplished by pressing a small pipette against the cell membrane (see Fig. 1). The pipette had a tip diameter of 1–3 μm and had smoothed edges to prevent cell damage. The inside of the pipette contained Ringer's solution and cholinergic agonist at low concentrations. The interior of the pipette was connected electrically by an Ag/AgCl electrode to a virtual ground circuit which clamped the inside of the pipette to ground and also provided a voltage output signal proportional to the current flowing through the pipette. Under appropriate conditions, which will be specified below, this current was equal to the membrane current, crossing the patch of membrane under study.

The membrane potential of the muscle fiber was controlled by a conventional two microelectrode voltage clamp. This arrangement is schematized in Figure 1. With membrane currents in the range of picoamperes the cell interior can be considered isopotential, and the patch is therefore "space clamped" even without the microelectrode clamp circuit. The only function of the voltage clamp is to set the patch-membrane voltage to values different from normal resting potential. In fact, single channel records can be obtained by just placing a single pipette onto a muscle fiber (see Fig. 6).

Similar pipette arrangements have been used before in various configurations and for different purposes (Pratt and Eisenberger, 1919; Strickholm, 1961; Frank and Tauc, 1963; Neher and Lux, 1969; Fishman, 1975).

The Equivalent Circuit

The region around the cell and pipette is a complicated volume conductor, but for a simplified treatment certain sections of electrolyte may be lumped into equivalent resistors (see Strickholm, 1961, for a more complete and detailed discussion of this topic). This is shown in Figure 2, where the internal resistance of the patch pipette is shown as R_p. The resistance of the shunt pathway under the seal of the electrode is R_{sh}, while the resistance from the edge of the seal to the bath ground is R_o. The exact separation into R_{sh} and R_o is arbitrary, but this is irrevelant to the argument below since R_o is much less than R_{sh} and, in any case, R_o and R_{sh} usually appear as their sum. The membrane patch itself has a very high impedance relative to these resistances and can be considered to be an ideal current source. (A patch of area 10 μm^2 has a capacitance in the range 0.1 to 1 pF and a resistance in the range 10^{10} Ω, while R_p is on the order of 3–5 MΩ and $R_{sh} \approx 15-45$ MΩ.) The current densities and absolute current values (< 10 pA) involved in these studies are so small that voltage drops across R_p, R_{sh} or R_o are negligible with respect to the transmembrane voltage. Thus, the patch of membrane is under voltage clamp conditions, since the potential inside is clamped by the intracellular microelectrodes, and extracellular voltage drops are in the μV range.

Fidelity of Current Measurement is Determined by the Ratio R_p/R_{sh}. When a channel opens in the membrane

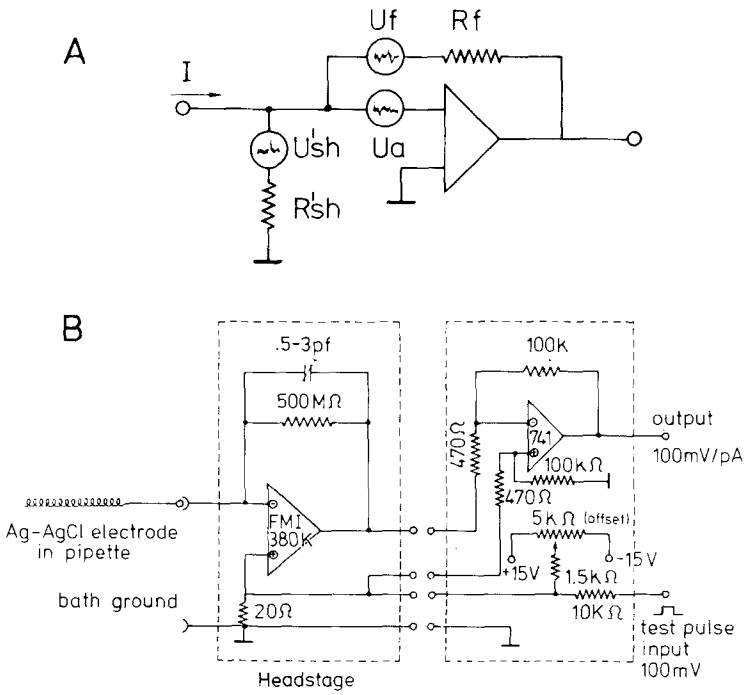

Fig. 3
(A) Simplified equivalent circuit with noise sources. The series combination of R_p, R_{sh} and R_o is represented by an equivalent resistor R'_{sh}. The possible sources of noise under consideration are: U_f the Johnson noise of the feedback resistor R_f; U_a the amplifier input voltage noise and U'_{sh} the Johnson noise of the equivalent shunt resistor. Input current noise of the amplifier is negligible for the module chosen. **(B)** Circuit diagram of the virtual ground circuit. The amplifier (a Function Modules 380 K, or Analog Dev. 515 or Burr Brown 3523) was chosen for low input current noise (< 0.1 pA at 200 Hz bandwidth) and the lowest possible voltage noise. The feedback resistor R_f used was 500 MΩ, which limited bandwidth to approx. 400 – 600 Hz. For higher bandwidth R_f can be chosen lower (> 100 MΩ), without appreciable deterioration of noise figure. The noninverting input is used for balancing any difference in electrode potentials and to supply, if desired, a 200 μV test pulse for determination of pipette resistance. An additional amplification stage measures the voltage drop across the feedback resistor and sets the output sensitivity to 100 mV/pA

patch, it can be considered to inject a current I to point A of the equivalent circuit (Fig. 2). This current will flow to ground through two pathways: a shunt current (I_{sh}) under the lip of the pipette and a pipette current (I_p) which flows through the virtual ground circuit, resulting in a voltage output signal. From the simplified equivalent circuit,

$$I_{sh} = \frac{R_p}{R_p + R_{sh} + R_o} I. \tag{1}$$

Thus, the relative error introduced by the shunt current is

$$\frac{I_{sh}}{I} = \frac{R_p}{R_{sh} + R_o + R_p} \approx \frac{R_p}{R_{sh}}. \tag{2}$$

A basic condition is, then, that the internal resistance of the patch electrode must be small compared to the seal (or shunt) resistance. An additional problem occurs if a channel opens under the lip of the electrode, part way across the shunt resistance. If that is the case, the relative error will be increased since part of R_{sh} appears as R_p and the numerator in eqn. (2) approaches the denominator. This problem will be discussed below.

Background Noise is Dominated by R_{sh}. The equivalent circuit of Figure 2 is redrawn in Figure 3A to indicate the major noise sources, apart from endogenous membrane noise. For simplicity, the series combination of $R_o + R_{sh} + R_p$ (and its associated Johnson voltage noise) has been lumped together and termed R'_{sh} (and U'_{sh}), since only this combination appears in the expressions. The other noise sources are the internal voltage noise of the virtual ground amplifier U_a and the noise in the feedback resistor U_f. The amplifier *current* noise is small and has been neglected. For zero input current, a noise output voltage signal appears which is (see Fig. 3A)

$$U_{out} = -U_a\left(1 + \frac{R_f}{R'_{sh}}\right) + U'_{sh}\frac{R_f}{R'_{sh}} + U_f. \tag{3}$$

This output signal will be interpreted as a membrane current noise signal of

$$I_n = \frac{U_{out}}{R_f} \approx -\frac{U_a}{R'_{sh}} + \frac{U_{sh}}{R'_{sh}} + \frac{U_f}{R_f} \tag{4}$$

(Note that $R_f = 500\,\text{M}\Omega$, so $R_f \gg R'_{sh}$.) The individual noise sources can be considered as statistically independent, such that their noise powers add. Thus,

$$\sigma_I^2 = \frac{\sigma^2_{U_a}}{R'^2_{sh}} + \frac{\sigma^2_{U'_{sh}}}{R'^2_{sh}} + \frac{\sigma^2_{U_f}}{R_f^2} \tag{5}$$

where σ_I^2, $\sigma^2_{U_a}$, $\sigma^2_{U'_{sh}}$ and $\sigma^2_{U_f}$ are the variances of output current, amplifier voltage noise, shunt resistor noise, and feedback resistor noise respectively. The second and third terms are the "current" Johnson noise contributions from the shunt and feedback resistors. Since $R_f \gg R'_{sh}$ the second (shunt resistance) term will be larger than the third one. Examining the first and second terms, it can be seen that their relative importance depends on the inherent amplifier voltage noise

power (independent of R'_{sh}) and the shunt resistor noise power (which increases as R'_{sh}). With the amplifier chosen (FMI 380 K), the second term dominates when $R'_{sh} > 1\,M\Omega$. Thus, for any reasonable value of shunt resistance ($10\,M\Omega < R'_{sh} < 50\,M\Omega$) the dominating noise source is the Johnson noise of R'_{sh}. The noise variance of R'_{sh} increases linearly with R'_{sh}, however, it is divided by R'^2_{sh} in the current measurement [eqn. (5)]. Thus, for low background noise, R'_{sh} should be as high as possible. To observe single channels of 2 pA amplitude, the background r.m.s. noise should be less than 0.5 pA. With a bandwidth of 200 Hz, this requires $R'_{sh} > 20\,M\Omega$.

It should be pointed out, that in the above case the residual background noise is just the Johnson noise of the signal source (the patch of membrane, shunted by a leak). This is the minimum possible noise for the given experimental situation. The result of $R_{sh} > 20\,M\Omega$ can be generalized: For any attempt to measure events of similar amplitude and duration, the impedance of the signal source (the input impedance of a cell or the impedance of a membrane-shunt-combination) should be 20 MΩ or larger. This situation may be contrasted with other instances of fluctuation analysis where increasing membrane area can be used to increase signal noise power above a fixed level of instrumentation noise.

Requirements for High Resolution Current Measurement

There are a number of considerations that must be taken into account in performing the actual experiments. The first two are dictated by the analysis of the equivalent circuit (see above).

1. The seal should be as high as possible: $R_{sh} > 20\,M\Omega$.

2. The shunt resistance should be larger than the pipette resistance: $R_{sh}/R_p > 5$.

In addition, two further properties are required for the data analysis:

3. There must be a sufficiently low frequency of events (a small number of simultaneously open channels).

4. The events must have slow time courses so that bandwidth of the recording apparatus can be limited to reduce background noise.

We outline here the procedures used to reach the above objectives, and than discuss the experimental details:

1. The critical factors in achieving a good seal are the tip geometry of the patch pipette, the closeness of the approach of the pipette to the membrane, and mechanical support of the muscle fiber. Enzymatic treatment was essential for a close approach of the pipette to the membrane.

2. In order to increase the ratio of the seal resistance to the pipette resistance it is necessary to achieve the best possible seal and to prepare patch pipettes with a steep final taper to minimize R_p.

3. To obtain a low frequency of events, experiments were done on extrajunctional regions of denervated skeletal muscle fibers, which have a low receptor density. (Alternatively, a proportion of the receptors could be inactivated by agents such as α-bungarotoxin.) During an experiment various sites were tested until one with an appropriate frequency of events was found. Small inner diameter pipettes ($1-3\,\mu m$) were used to limit the membrane area of the patch, while a low concentration of agonist ($< 10^{-6}\,M$) was used to further reduce the frequency of events.

4. In order to achieve events of sufficiently slow time course, experiments were done at low temperature ($6-12°\,C$). Also, the receptors on denervated extrajunctional regions showed slower closing rates than junctional receptors (Katz and Miledi, 1972; Neher and Sakmann, 1976b; Sakmann, 1975). Finally, most experiments were performed using suberyldicholine (Sub) as agonist, since channels activated by suberyldicholine have a longer mean open-time than those opened by other agonists (Katz and Miledi, 1973; Colquhoun et al., 1975).

The shape of the pipette is of particular importance for the success of the experiment. A delicate compromise between various shape parameters had to be found, since some of the requirements listed above are conflicting. For instance, decreasing tip diameter improves the shunt resistor R_{sh}, however, it makes it more difficult to obtain a high ratio R_{sh}/R_p.

The wall thickness of the pipette has a dual influence: Increasing wall thickness increases R_{sh} and concomitantly improves signal to noise-ratio; at the same time it creates a very unfavourable relation between the area of the patch (inside the pipette) and the area under the seal. As a result, an appreciable fraction of channels are activated part way across R_{sh}. Their current contributions are difficult to interpret (see below). As a compromise, pipettes were used with an internal diameter of approximately $1-3\,\mu m$ and shapes as illustrated in Figure 4. These pipettes had resistances between 2 and 4 MΩ (Ringer filled) which increased to 20 to 40 MΩ when approaching a fiber.

Experimental Details

Construction of the Patch Pipettes. Rawlings were pulled on a conventional puller using thin-walled glass

tubing (Kimax capillaries, i.d. ≈ 1.3 mm, o.d. ≈ 1.8 mm). Patch electrodes were prepared from them on a microforge. Part of the following description is the standard routine for pulling microelectrodes on a microforge, adapted for extra steep taper: The first step was to shape the tips of the rawlings into a hook which was used for suspension of a 0.8 g weight. Then, the hot microforge filament was brought near the shank of the vertically mounted pipette, where the o.d. of the pipette was about 0.2 mm. The pipette was allowed to be drawn out by the weight, until a constriction with a sharp taper was produced. The final o.d. was about 10–20 μm. A stream of air was then passed over the filament and pipette, to localize heating to a very short length of the pipette. The current through the filament was decreased stepwise, and concomitantly the filament was brought closer to the narrowest point of the constriction. The heating current was always kept at the lowest value which produced further constriction. This resulted in a spontaneous square break at about 5–10 μm diameter. The tips were fire polished by carefully bringing them near the hot filament with the current of air still on (the pipette now being mounted horizontally). The air stream localized the heat such that only the final 5–10 μm melted and further constricted. This gave the typical tip shapes as illustrated in Figure 4. Attempts were made to increase the seal resistance by coating the pipette tips with Sylgard (Dow-Corning), either cured or uncured, but this did not result in a significant improvement. Similarly, attempts to reverse the surface charges of the glass by treatment with poly-L-lysine or protamine were without striking results. About 50% of all pipettes were usable, the rest having various defects (too large or small diameters, uneven breakage, spurs of glass protruding from the tip and so forth).

Pipettes were filled by immersing the tips in the desired solution until the meniscus had risen high enough so that the electrode could be back-filled with a 27 gauge hypodermic needle. All solutions were filtered through a membrane filter (Millipore 0.45 μm pore size) immediately before use. This filtration was critical, to remove dust particles which otherwise would clog the tip.

It was possible to refill pipettes with new solutions by removing the shank solution with a fine hypodermic and then flushing the tip by sucking up solution repetitively using a syringe and fine tubing connected to the tip of the pipette.

Pipettes sometimes "clogged": R_p would increase and it would not be possible to achieve a good seal after withdrawing the pipette from a muscle fiber. It was possible to "clean" a pipette by pressing it against a ball of cured Sylgard on the tip of the hook used to support the muscle fiber (see below and Fig. 1). This procedure also turned out to be a good check for pipette performance: Pipettes, touching a Sylgard surface, should seal immediately and completely without mechanical pressure involved. Behaviour contrary to that was an indication for irregularities on the pipette tip.

Recording Apparatus and Mechanical Setup. A conventional two micropipette voltage clamp was used to control the membrane potential of the muscle fiber. The virtual ground circuit for measurement of pipette current is given in Figure 3B. Its amplifier was mounted as close to the pipette as possible, on the head of a motor-driven micromanipulator (Rodenstock, München). The rest of the patch clamp circuitry (Fig. 3B) was placed in a separate box away from the preparation.

The input from the patch electrode was made to a BNC connector; the female BNC connector was modified so that an Ag/AgCl wire passed through a plastic pin vise. The patch electrode was passed over the chlorided wire and secured in the pin vise. The assembly was plugged directly into the amplifier box. To reduce electrical pickup, a sliding aluminium sleeve could be adjusted to shield much of the length of the pipette. We also found that it was necessary to protect the chlorided portion of the silver wire with a thin polyethylene tube. This prevented damage when sliding on the pipette, eliminating a major source of drift. The Ag/AgCl wire was always kept immersed in Ringer's solution between experiments and was not allowed to dry out at any time. We used a large surface area sintered Ag/AgCl bath electrode (Annex Research, Santa Ana), to reduce slow changes in pipette current (10–50 pA, over minutes), probably due to polarization when smaller area ground electrodes were used.

Pipettes were filled with enough solution so that, when the tips were immersed in the bath, there was a steady slow outflow of solution, insuring that the agonist concentration at the tip was not reduced by dilution.

The Preparation. Frog cutaneous pectoris muscles were denervated by removing a 3–7 mm length of the N. pectoralis communis and ligating both ends in the armpit, close to where this nerve leaves the N. spinalis III (Ecker et al., 1899). Muscles had been denervated for 4–6 weeks. They were dissected down to about a fiber bilayer, then treated with enzyme (Betz and Sakmann, 1973). Enzymes were dissolved in normal Ringer's solution. First 0.2% Collagenase (Sigma, type I), then 0.02% protease (Sigma, VII) were flowed over the muscle at a rate of about 10 ml/h for 80 and 40 min, respectively. Prolonged enzyme treatment led to freely floating fibers as recently described (Bekoff and Betz, 1977). In our experiments, however, the enzyme action was restricted to the middle part of the muscle by

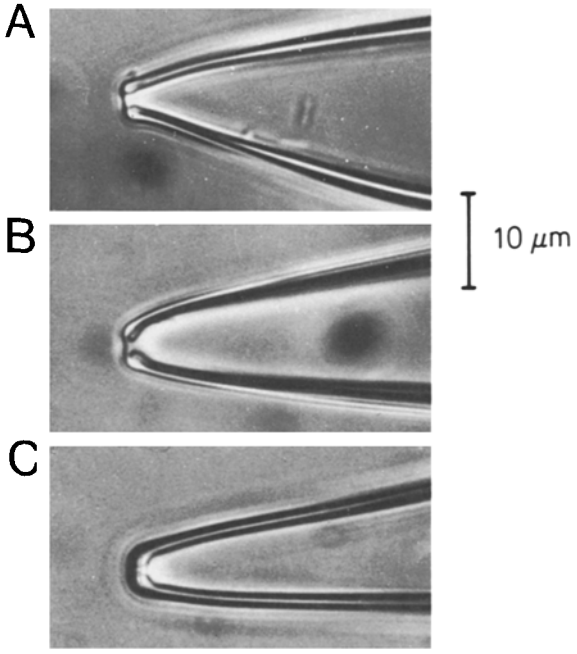

Fig. 4A–C. Water immersion micrograph of fire polished pipettes. The different pipettes represent relatively thin-walled (**A**) and thick-walled (**B** and **C**) cases. The actual wall thickness may not be larger in **B** compared to **A**. However, **B** was made for extra inwand curvature right at its tip, which gave a larger seal area in the experiments. The internal resistance of pipette **A** was 1.9 MΩ which increased to 25 MΩ upon touching the muscle surface. Pipette **B** had a resistance of 2.8 MΩ. This kind of pipette could obtain a seal resistance of up to 35 MΩ. Pipette **C** was an extreme example of the "thickwalled" case in which the ratio of seal area to the area of the opening was very large due to a very small inner diameter. The recordings of Figure 6 were obtained with this pipette. It had an internal resistance of 4 MΩ which increased to 40 MΩ upon establishment of a seal

flowing plain Ringer's at a faster rate from a pipette located upstream of the enzyme-delivering pipette. With progressing enzyme treatment stretch on the fibers had to be reduced in order to prevent breakage of the fibers. Also, TTX at a concentration of approximately 10^{-8} M had to be added. After enzyme treatment, the muscles were further dissected down to a fiber monolayer.

The duration of the collagenase treatment had to be varied from preparation to preparation depending on the extent of connective tissue. The following was used as a criterion for sufficient collagenase treatment: Before switching to protease it should be possible to separate individual fibers from one another by a jet of Ringer's delivered through a Pasteur pipette.

Experiments on rat muscle fibers were done on diaphragm and omohyoid muscles. Muscles were denervated for 5–10 days. Enzyme treatment consisted of a 3 h incubation of muscles in 0.07% collagenase (Sigma, type I) in Trowells T 8 medium (Flow Laboratories) at room temperature. Protease treatment had to be omitted since this resulted in a rapid loss of resting potential and clotting of fibers. The incubation medium was bubbled continuously with a 95% O_2 and 5% CO_2 gas mixture. Before enzyme treatment the muscle was dissected down to a few layers in order to ease enzyme access.

Fibers were observed using a 16× long working distance Nomarski objective (5 mm, McBain Instruments) at a final magnification of 200×. Alternatively a stereo lens (Wild M 5) with dark field illumination was used. The bath temperature was controlled by two Peltier devices and was monitored by a small thermistor placed near the muscle. Standard frog (Anderson and Stevens, 1973) or rat Ringer (Liley, 1956) was used, except where indicated otherwise. Suberyldicholine was a gift from J. Heesemann (Max-Planck-Institut, Göttingen).

An important experimental aid was a glass hook, prepared in the microforge, which was mounted on a micromanipulator and used to pick up and steady the muscle fiber. The hook prevented the fiber from rolling and sliding off the intracellular electrodes. It also carried a small ball of Sylgard on its tip, used to clean the patch electrode as described earlier.

The procedure was to pick up a fiber with the hook and insert the two micropipettes close to each other (within 100 μm) on one side of it and within 100 μm of the hook (see Fig. 1). The patch electrode was brought down on the other side of the hook, again within 50 μm of it. The patch electrode usually dimpled the surface of the fiber before a good seal was obtained.

Patch electrode signals were monitored on an oscilloscope and recorded on an FM tape recorder.

Signals were replayed for analysis through a four-pole low pass filter with Bessel characteristics, the corner frequency of which was adjusted between 50 and 600 Hz.

Performance of the Patch Clamp Method

Tests of Resolution

Background Noise is a Function of Shunt Resistance. Analysis of the equivalent circuit (Figs. 2 and 3) has indicated that noise performance of the patch clamp method should mainly depend on the magnitude of the series combination of access resistance R_o, shunt resistance R_{sh}, and pipette resistance R_p. It was shown that under a wide range of conditions the background noise should be exactly the Johnson noise of this combination (termed R'_{sh}).

In the experiments, the value of R'_{sh} was monitored during establishment of contacts between pipette and membrane. This was done by applying 200 μV square

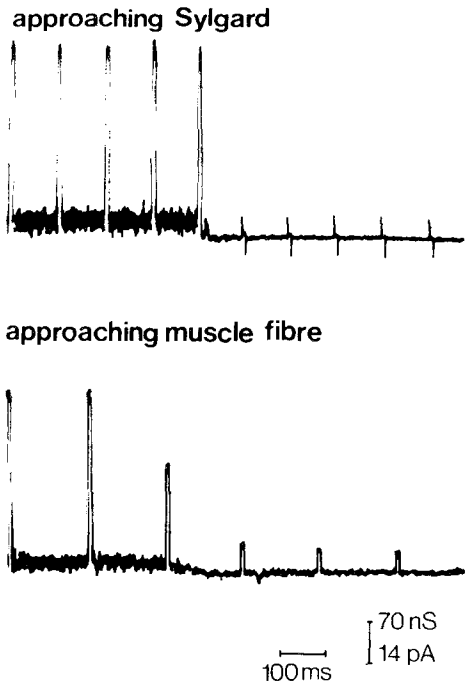

Fig. 5. Current recording during closure of a pipette tip. The amplitude of the repetitively occurring test-pulses are proportional to the conductance between pipette interior and bath ground. When contact is established, conductance – and concomitantly background noise – is decreased (see text). The seal is perfect when a pipette is touched to a Sylgard surface. However, it is incomplete, even after extensive enzyme treatment, if the pipette is brought in contact with a biological membrane

pulses to the noninverting input of the virtual ground amplifier, and recording the pipette current I_p (see Fig. legend 3). I_p was then proportional to $1/R'_{sh}$. Figure 5 shows two such experiments. In the upper record a pipette was lowered towards a surface of cured Sylgard (at 400 Hz bandwidth). Before contact R'_{sh} was small (3.5 MΩ, – pulses of pipette current were large), and current noise was large, approx. 1.5 pA (rms). Upon contact, an almost perfect seal was established and R'_{sh} became very large. The impedance between pipette interior and bath in this case was mainly capacitive, with a resistive component in the range 500 MΩ – 1 GΩ. Correspondingly the background noise was very small ($\simeq$ 0.2 pA) being mainly determined by the Johnson noise of the feedback resistor and current noise of the amplifier.

In the lower record the same pipette was lowered towards a muscle fiber (at approx. 200 Hz bandwidth). In this case the seal was incomplete, approaching a value between 35 – 40 MΩ. Concomitantly background noise decreased to a final value of 0.45 pA (rms). Shortly after contact a channel opening occurred in the recording of Figure 5, which under the conditions of this recording ($\simeq -80$ mV resting potential) produced only a very small downward deflection. It can be seen, however, from the record, that a good seal and its associated decrease in background noise is essential for resolving single channels.

In 8 measurements of background noise with bandwidths between 400 Hz and 60 Hz and values of R'_{sh} between 4 and 40 MΩ the rms-value was within 30 % of the Johnson noise contribution of R'_{sh}.

Bandwidth. The frequency response of the measurement was set by the RC-time constant of the feedback resistance R_f and stray capacitances across its ends. With an R_f of 500 MΩ, a bandwidth of 600 – 900 Hz could be obtained, which however, had a tendency to peak around the cutoff frequency. Therefore an air capacitor of approx. 0.3 – 0.5 pF was introduced parallel to R_f which gave a smooth rolloff at 600 Hz. This bandwidth was measured with proper loading of the circuit input, i.e. with a pipette connected and a normal seal established. In most experiments bandwidth was limited, however, by a subsequent filter stage for better signal to noise ratio.

Some Properties of Acetylcholine Receptor Channels

Experiments were performed with both 6 weeks denervated frog cutaneous pectoris muscles and with 7 days denervated rat diaphragm muscles. The frog results have been described before (Neher and Sakmann, 1976a, b; Neher and Steinbach, 1978). A further example is given in Figure 6. Contrary to the normal procedure this measurement was taken from an unclamped fiber, just by placing a pipette (pipette from Fig. 4C) onto a fiber without intracellular microelectrodes. A low K^+-Ringer was used in this experiment to increase resting potential. Also, Ca^{2+} was replaced by Mg^{2+}, which gave a more stable preparation (see Fig. legend 6). Resting potential was between –95 and –100 mV, as can be inferred from measurements taken after the recording. The illustration compares two cases in the absence (upper half) and presence (lower half) of d-Tubocurarine (dTC) in the Ringer bath (see below).

An example of a recording from rat diaphragm is given in Figure 7. It can be seen in Figures 6 and 7 that single channels contribute square wave-like currents with a stochastically varying pulse length. The pulse amplitude increases with membrane hyperpolarization (Fig. 7), and is consistent with a linear I – V-relationship.

Occasionally current levels higher than the single open channel level occur (see second trace in Fig. 6). These events seem to be statistical superpositions of two or more independent channels. The probability of finding a certain number of channels open simultaneously follows a Poisson distribution, as shown in

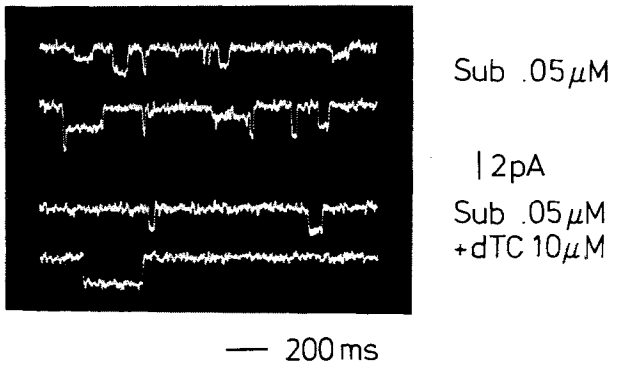

Fig. 6. Four recordings from an unclamped frog cut. pectoris preparation with an extremely "thickwalled" pipette (pipette C of Fig. 4) at 11 C. Resting potential was approx. −95 to −100 mV (see text), suberyldicholine was present at 50 nM inside the pipette in all four traces. Low K^+, low Ca^{2+}-Ringer was used for high resting potential and better mechanical stability (Composition (mM): 117 NaCl; 0.5 KCl; 1.8 $MgCl_2$; 2.16 Na_2HPO_4; 0.85 NaH_2PO_4). In the lower two records the bath (not the pipette!) contained in addition 10 μM d-tubocurarine (dTC). Note low frequency of events and uniform step size in these two traces. Recording bandwidth: 180 Hz

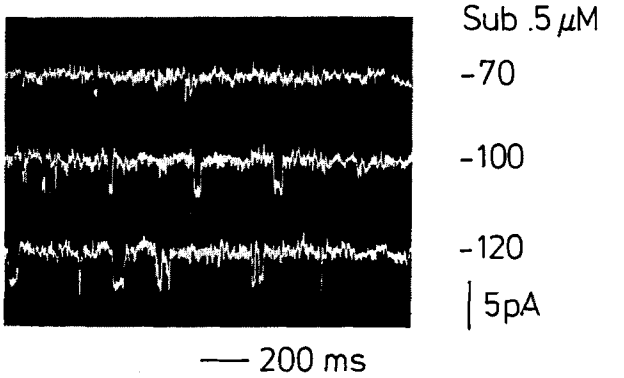

Fig. 7. Recordings from a rat diaphragm fibre clamped to −70 mV, −100 mV, and −120 mV at 12° C. A "thinwalled" pipette was used, such that current steps were relatively uniform. Step sizes increased with hyperpolarization indicating an approximately linear I-V-relationship and an equilibrium potential around 0 mV. Quantitative analysis of amplitudes is complicated, however, due to some scatter in step sizes.

Table 1. Statistics of the number of simultaneously open channels: The proportions of total recording time when a given number v of channels were open are compared to the predicted probabilities P_v, assuming a Poisson process. The upper value in each pair is the experimental value, while the lower number is the Poisson prediction. Frog cut. pector.; 0.1 μM Sub; 8° C. $< v >$ is the mean number of channels open at a given moment, averaged over the whole record. The Poisson prediction is based on $< v >$

Membrane pot	Number of events	$< v >$	P_0	P_1	P_2	P_3
−120	125	0.418	0.652 0.658	0.287 0.275	0.050 0.056	0.01 0.006
−120	119	0.214	0.805 0.807	0.175 0.172	0.018 0.0184	0.0003 0.001
−120	128	0.231	0.793 0.793	0.182 0.183	0.023 0.0212	0.0005 0.0016
−120	61	0.158	0.84 0.85	0.144 0.135	0.007 0.016	
− 90	63	0.0532	0.947 0.948	0.051 0.050	0.0011 0.0013	
−120	87	0.2461	0.7826 0.782	0.188 0.192	0.0287 0.0236	
−145	52	0.139	0.87 0.87	0.1203 0.121	0.00936 0.008	
−120[a]	98	0.037	0.9638 0.9636	0.0353 0.0356	$8.4 \cdot 10^{-4}$ $6.6 \cdot 10^{-4}$	

[a] Rat diaphragm, 0.5 μM Sub, 12 C.

Table 1. Note that there is no systematic deviation from the Poisson prediction. Looking at the probabilities for the higher levels, (P_1, P_2, P_3), which are most indicative for deviations from a Poisson distribution, one can see that 8 observed probabilities are larger than the Poission prediction and 11 are smaller.

The Opening Time Course is Fast. It was mentioned in the introduction that single channel contributions here and also in several examples of artificial systems look like square pulses i.e. the transition from the closed state to a steady open state is fast compared to the mean lifetime of the open state. In order to obtain an upper limit to the duration of the transition, we photographed a number of these transitions at good time resolution and measured rise times (time between 10% and 90% completion of the steps). A mean value of 0.51 ms was obtained at 8° C. This indicates a time constant of 0.23 ms or a cutoff frequency between 600 and 700 Hz. This is just the bandwidth of the recording apparatus. We conclude, therefore, that transitions are probably faster and what we observe is the response of the measuring system to a square pulse.

Thick-Walled Pipettes Distort Channel Amplitude Histograms. The highest signal to noise ratio was obtained with thick-walled pipettes as shown in Figure 4B and C. However, it was observed that under these conditions single channel amplitudes were nonuniform. In addition to the fullsized channels, the amplitude of which correspond to the known channel conductance of 25−35 pS, there was a large number of smaller events (see Fig. 6, first two traces and Fig. 1 in Neher and Steinbach, 1978). Figure 8 shows a step size histogram from such a recording which is contrasted in part B to the case of a recording with a thin-walled

pipette of the kind shown in Figure 4A. A straightforward explanation for this effect is offered by the hypothesis that the small-sized electrical events are located under the pipette rim, partway across the seal (see methods section). This might occur although there is a gradient of agonist between the pipette interior and the external bath which preferentially activates channels in the center of the patch. The hypothesis can be tested by applying curare to the bath medium. Curare has been shown by noise analysis to decrease the number of available channels, but to leave the conductance of the remaining ones constant (Katz and Miledi, 1972). Curare should preferentially block receptors furthest outside of the seal area and therefore restore a more uniform channel size. Figure 6 shows recordings in the absence and presence of curare at 10 μM concentration. Curare, if present, was added to the external bath only, not to the pipette solution. The upper two traces, taken immediately before perfusion of the chamber with curare-solution, are marked by a relatively high frequency of events with nonuniform step sizes. The baseline is irregular and noisy, probably, due to channel currents too small in amplitude to be recognized as square pulses. The lower two traces, taken from the same fiber and the same membrane patch within a minute after curare perfusion show a largely decreased frequency of channel openings, quite uniform step sizes and a straight baseline. Figure 9 shows step size histograms of longer sections from the same two recordings in the absence (part A) and in the presence of curare in the outer bath (part B). The difference between the histograms supports our hypothesis. We conclude, that step sizes are indeed relatively uniform. Thick-walled pipettes, although superior in signal to noise ratio, have the disadvantage of recording a substantial number of events from the badly defined seal area.

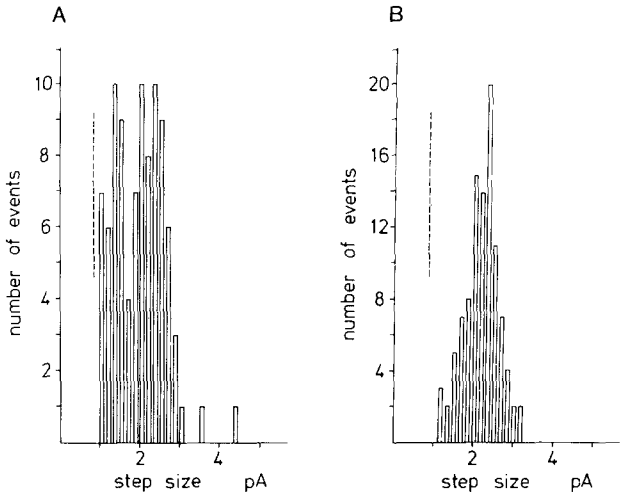

Fig. 8A and B. Histograms of step sizes: Comparison between a recording using a "thickwalled" pipette (**A**) versus one with a "thinwalled" pipette (**B**). The histograms give the relative frequency of occurrence (ordinate) of current steps of a given amplitude (abscissa) at a membrane potential of −80 mV; 8° C. The histograms are not evaluated below 1 pA (broken line) which is considered the limit of resolution. Note more uniform step sizes in the case of "thinwalled" pipettes. The histograms are based on 98 (part **A**) and 102 (part **B**) determinations of step size

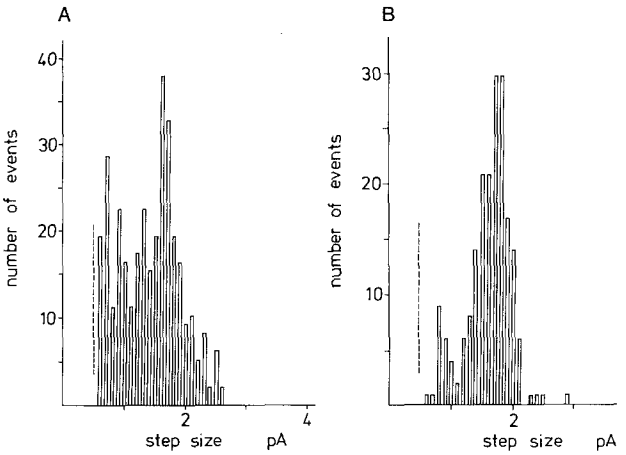

Fig. 9A and B. Histograms of step sizes: Comparison between a recording before (case **A**) and after (case **B**) addition of 10 μM curare to the Ringer bath. Analysis of records, 1 to 2 min in length, subsections of which were taken for Figure 6. See Figure legend 6 for conditions. Note relative suppression of small amplitude steps in the presence of curare. The histograms are based on 335 (part **A**) and 194 (part **B**) determinations of step size

Discussion

We have shown that the extracellular patch clamp can be reliably used to detect extremely small currents flowing through biological membranes. At present the technique has limitations, however, in terms of the frequency, duration and amplitude of events which can be studied. We emphazised the problems that arise from the fact that current traversing the membrane, which is covered by the wall of the pipette, is poorly defined in terms of the measurement. We would like to point out that analogous problems might arise with a number of widely used techniques where sucrose, vaseline or plastic separations are used to subdivide membrane areas. Extrajunctional acetylcholine receptors of amphibian and mammalian muscles were studied; the method should be readily extended to other chemically activated membrane channels and possibly to voltage-sensitive channels as well.

We have formed the following picture of acetylcholine receptors in the extrajunctional regions of

denervated vertebrate skeletal muscle fibers: a channel opens and closes rapidly and has a constant conductance when open. The current voltage relation is approximately linear. Neighbouring channels do not interact, since the probability of finding a given number of channels open at a time follows a Poisson distribution. This picture is identical with the one earlier used by Anderson and Stevens (1973) to analyze their membrane current fluctuation data.

Acknowledgement. Part of this work was conducted in the laboratory of Dr. Ch. F. Stevens, at the Physiology Department of Yale University. E. N. was supported during that time by NS grant No. 12961 to Dr. Stevens. J. H. S. was supported by a fellowship of the Muscular Dystrophy Association. We want to thank Dr. Stevens for his support and encouragement.

References

Anderson, C. R., Stevens, C. F.: Voltage clamp analysis of acetylcholine produced end-plate current fluctuations at frog neuromuscular junction. J. Physiol. (Lond.) **235**, 655–691 (1973)

Bean, R. C., Shepherd, W. C., Chan, H., Eichner, J. T.: Discrete conductance fluctuations in lipid bilayer protein membranes. J. Gen. Physiol. **53**, 741–757 (1969)

Bekoff, A., Betz, W. J.: Physiological properties of dissociated muscle fibres obtained from innervated and denervated adult rat muscle. J. Physiol. (Lond.) **271**, 25–40 (1977)

Betz, W., Sakmann, B.: Effects of proteolytic enzymes on function and structure of frog neuromuscular junctions. J. Physiol. (Lond.) **230**, 673–688 (1973)

Colquhoun, D., Dionne, V. E., Steinbach, J. H., Stevens, C. F.: Conductance of channels opened by acetylcholine-like drugs in muscle end-plate. Nature **253**, 204–206 (1975)

Ecker, A., Wiedersheim, R., Gaupp, E.: Anatomie des Frosches, 2. Abth. Braunschweig: Vieweg 1899

Fishman, H. M.: Patch voltage clamp of squid axon membrane. J. Membrane Biol. **24**, 265–277 (1975)

Frank, K., Tauc, L.: Voltage-clamp studies of molluscan neuron membrane properties. In: The cellular functions of membrane transport. (Hoffmann, J., ed.). Englewood Cliffs, New Jersey: Prentice Hall, Inc. 1963

Gordon, L. G. M., Haydon, D. A.: The unit conductance channel of alamethicin. Biochim. Biophys. Acta **255**, 1014–1018 (1972)

Hladky, S. B., Haydon, D. A.: Ion transfer across lipid membranes in the presence of Gramicidin A. I. Studies of the unit conductance channel. Biochim. Biophys. Acta **274**, 294–302 (1972)

Katz, B., Miledi, R.: The statistical nature of the acetylcholine potential and its molecular components. J. Physiol. (Lond.) **224**, 665–699 (1972)

Katz, B., Miledi, R.: The characteristics of 'endplate noise' produced by different depolarizing drugs. J. Physiol. (Lond.) **230**, 707–717 (1973)

Liley, A. W.: An investigation of spontaneous activity at the neuromuscular junction of the rat. J. Physiol. (Lond.) **132**, 650–656 (1956)

Neher, E., Lux, H. D.: Voltage clamp on Helix pomatia neuronal membrane; Current measurement over a limited area of the soma surface. Pflügers Arch. **311**, 272–277 (1969)

Neher, E., Sakmann, B.: Single-channel currents recorded from membrane of denervated frog muscle fibres. Nature **260**, 779–802 (1976a)

Neher, E., Sakmann, B.: Noise analysis of drug induced voltage clamp currents in denervated frog muscle fibres. J. Physiol. (Lond.) **258**, 705–729 (1976b)

Neher, E., Steinbach, J. H.: Local anesthetics transiently block currents through single ACH-Receptor channels. J. Physiol. **277**, 153–176 (1978)

Pratt, F. H., Eisenberger, J. P.: The quantal phenomena in muscle. Am. J. Physiol. **49**, 1 (1919)

Sachs, F., Lecar, H.: Acetylcholine-induced current fluctuations in tissue-cultured muscle cells under voltage clamp. Biophys. J. **17**, 129–143 (1977)

Sakmann, B.: Noise analysis of acetylcholine induced currents in normal and denervated rat muscle fibres. Pflügers Arch. **359**, R89 (1975)

Strickholm, A.: Impedance of a small electrically isolated area of the muscle cell surface. J. Gen. Physiol. **44**, 1073–1088 (1961)

Received December 23, 1977